

# Quadratic and Higher Order Time-Frequency Analysis Based on the STFT

*LJubiša Stanković*

The oldest, simplest, and most commonly used tool for time-frequency (TF) analysis of a signal  $x(t)$  is the spectrogram, defined as a squared magnitude of the short time Fourier transform (STFT) [1]

$$F_x(t, f) = \int_{-\infty}^{\infty} x(t + \tau)w(\tau)e^{-j2\pi f\tau} d\tau, \quad (1)$$

where  $w(\tau)$  is a real-valued even lag window. Implementations (hardware and software) of this transform are already widely present in practice. The STFT is linear and very simple for realization. However, it has some serious drawbacks. The most important one lies in its low concentration in the TF plane, when highly nonstationary signals are analyzed. In order to improve TF representation, various quadratic distributions have been introduced. The most important member of this class is the pseudo Wigner distribution (WD)

$$W_x(t, f) = \int_{-\infty}^{\infty} w\left(\frac{\tau}{2}\right)w\left(-\frac{\tau}{2}\right)x\left(t + \frac{\tau}{2}\right)x^*\left(t - \frac{\tau}{2}\right)e^{-j2\pi f\tau} d\tau. \quad (2)$$

The WD itself has a drawback. Namely, in the case of multicomponent signals,  $x(t) = \sum_{p=1}^P x_p(t)$ , it produces emphatic cross-terms that can completely mask the auto-terms and make this distribution useless for analysis. This is why many other quadratic reduced interference distributions have been introduced (Choi-Williams, Zao-Atlas-Marks, Born-Jordan, Butterworth, Zhang-Sato...) [1], [Article 6.4]. The cross-terms reduction in these distributions is based on a kind of

Time-Frequency Signal Analysis and Processing, ed. B. Boashash, Elsevier, 2003.

the Wigner distribution smoothing, which inherently leads to the auto-terms degradation [11]. In contrast to these TF representations, which are focused on the preservation of marginal properties and the cross-terms reduction, the S-method (SM), which is the topic of this article, is derived with the primary goal to preserve the auto-terms quality as in the WD, while avoiding (reducing) the cross-terms. The software and hardware realization of this method is very efficient, since it is completely based on the STFT. The SM can, in a straightforward manner, be extended to the cross-terms free (reduced) realization of the higher order TF representations, time-scale representations, and multidimensional space/spatial-frequency representations.

## A. STFT Based Realization of the Quadratic Representations

### A.1 Basic S-Method Form

Relation between the STFT and the WD, [6],

$$W_x(t, f) = 2 \int_{-\infty}^{\infty} F_x(t, f + \theta)F_x^*(t, f - \theta)d\theta \quad (3)$$

has led to the definition of a TF representation, referred to as the S-method (SM),

$$SM_x(t, f) = 2 \int_{-\infty}^{\infty} P(\theta)F_x(t, f + \theta)F_x^*(t, f - \theta)d\theta. \quad (4)$$

The special cases of the SM are two most important TF distributions: 1) For  $P(\theta) = 1$  the WD follows,  $SM_x(t, f) = W_x(t, f)$ , and 2) For  $P(\theta) = \delta(\theta)/2$ , the spectrogram  $SM_x(t, f) = |F_x(t, f)|^2 = S_x(t, f)$  is obtained. By changing the width of window  $P(\theta)$ , denoted by  $2L_P$

( $P(\theta) = 0$  for  $|\theta| > L_P$ ), between these two extreme cases we can get a gradual transition from the spectrogram to the WD. The best choice of  $L_P$  would be the value when  $P(\theta)$  is wide enough to enable complete integration over the auto terms, but narrower than the distance between the auto-terms, in order to avoid the cross terms, Fig.1. Then, the SM produces the sum of the WDs of individual signal components, avoiding cross-terms.

**Proposition:** Consider the signal  $x(t) = \sum_{p=1}^P x_p(t)$ , where  $x_p(t)$  are monocomponent signals. Assume that the STFT of each component lies inside the region  $D_p(t, f)$ ,  $p = 1, 2, \dots, P$ . Denote the length of the  $p$ -th region along  $f$ , for a given  $t$ , by  $2B_p(t)$ , and its central frequency by  $f_{0p}(t)$ . The SM of  $x(t)$  produces the sum of the WDs  $W_{x_p}(t, f)$  of each signal component  $x_p(t)$ ,

$$SM_x(t, f) = \sum_{p=1}^P W_{x_p}(t, f), \quad (5)$$

if the regions  $D_p(t, f)$ ,  $p = 1, 2, \dots, P$ , do not overlap,  $D_p(t, f) \cap D_q(t, f) = \emptyset$  for  $p \neq q$  (meaning cross-terms free spectrogram), and if the width of the rectangular window  $P(\theta)$ , for a point  $(t, f)$ , is defined by  $L_P(t, f) = B_p(t) - |f - f_{0p}(t)|$  for  $(t, f) \in D_p(t, f)$ , and 0 elsewhere.

**Proof:** Consider a point  $(t, f)$  inside a region  $D_p(t, f)$ . The integration interval in (4), for the  $p$ -th signal component is symmetrical with respect to  $\theta = 0$ . It is defined by the smallest absolute value of  $\theta$  for which  $f + \theta$  or  $f - \theta$  falls outside  $D_p(t, f)$ , i.e.,  $|f + \theta - f_{0p}(t)| \geq B_p(t)$  or  $|f - \theta - f_{0p}(t)| \geq B_p(t)$ . For  $f > f_{0p}(t)$  and positive  $\theta$ , the integration limit is reached first in  $|f + \theta - f_{0p}(t)| \geq B_p(t)$  for  $\theta = B_p(t) - (f - f_{0p}(t))$ . For  $f < f_{0p}(t)$  and positive  $\theta$ , the limit is reached first in  $|f - \theta - f_{0p}(t)| \geq B_p(t)$  for  $\theta = B_p(t) - (f_{0p}(t) - f)$ . Thus, having in mind the interval symmetry, an integration limit which produces the same value of integral (4) as the value of (3), over the region  $D_p(t, f)$ , is given by  $L_P(t, f)$  in the Proposition. Therefore, for  $(t, f) \in D_p(t, f)$  we have  $SM_x(t, f) = W_{x_p}(t, f)$ . Since  $L_P(t, f) = 0$  for  $(t, f) \notin D_p(t, f)$ ,  $p = 1, 2, \dots, P$ .

**Note:** Any window  $P(\theta)$  with constant width  $L_P \geq \max_{(t,f)} \{L_P(t, f)\}$  produces

$SM_x(t, f) = \sum_{p=1}^P W_{x_p}(t, f)$ , if the regions  $D_p(t, f)$ ,  $p = 1, 2, \dots, P$ , are at least  $2L_P$  apart along the frequency axis, i.e.,  $|f_{0p}(t) - f_{0q}(t)| > B_p(t) + B_q(t) + 2L_P$ , for each  $p, q$  and  $t$ . This is the SM with constant window width (4). *If two components overlap for some time instants  $t$ , then the cross-term will appear, but only between these two components and for that time instants.*

The SM belongs to the general class of quadratic TF distributions, whose inner product form reads

$$\rho_x(t, f) = \int_{-\infty}^{\infty} \int_{-\infty}^{\infty} \tilde{G}(t_1, t_2) [x(t + t_1)e^{-j2\pi ft_1}] \times [x(t + t_2)e^{-j2\pi ft_2}]^* dt_1 dt_2. \quad (6)$$

If the inner product kernel  $\tilde{G}(t_1, t_2)$  is factorized in the Hankel form  $\tilde{G}(t_1, t_2) = 2w(t_1)p(t_1 + t_2)w(t_2)$ , then by substituting its value into (6), with  $P(-f) = \mathcal{F}_{t \rightarrow f}\{p(t)\}$ , we get (4). Note that the Toeplitz factorization of the kernel  $\tilde{G}(t_1, t_2) = 2w(t_1)p(t_1 - t_2)w(t_2)$  results in the smoothed spectrogram. The smoothed spectrogram composes two STFTs in the same direction, resulting in the distribution spread, in contrast to the SM, where two STFTs are composed in counterdirection, resulting in the concentration improvement, Fig.1, [5], [Article 9.1].

The SM kernel in Doppler-lag domain is given by  $c(\nu, \tau) = P(\nu/2) *_{\nu} A_{ww}(\nu, \tau)$ , where  $A_{ww}(\nu, \tau)$  is the ambiguity function of  $w(\tau)$ , and  $*_{\nu}$  denotes a convolution in  $\nu$ . Generally, this kernel is not a separable function.

### A.2 Other Forms of the S-Method in Quadratic Representations

**Time direction form** of the SM is

$$SM_x(t, f) = 2 \int_{-\infty}^{\infty} P(\tau) F_x(t + \tau, f) F_x^*(t - \tau, f) e^{-j4\pi f \tau} d\tau. \quad (7)$$

It results from the same analysis as (4), based on the frequency domain windowed WD,  $W_x(t, f) = \int_{-\infty}^{\infty} W(\theta/2)W(-\theta/2)X(f + \theta/2)X^*(f - \theta/2) \exp(j2\pi t\theta) d\theta$ .

**Fractional domain form:** The frequency and time direction forms of the SM can be generalized to any direction in the time-frequency

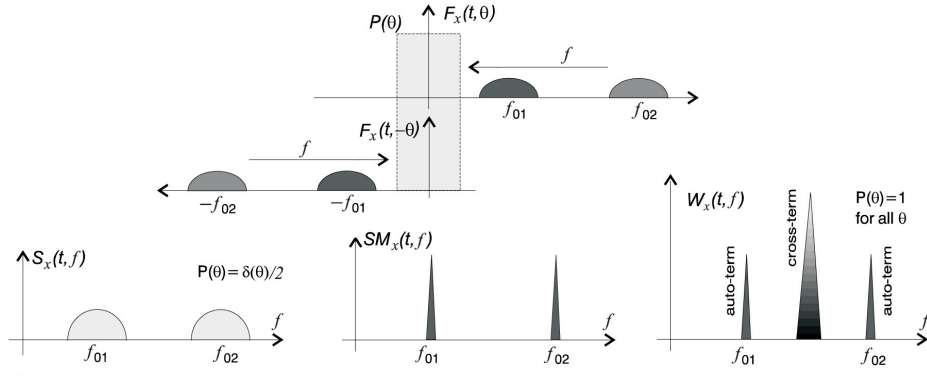


Fig. 1. Illustration of the SM calculation including two special cases: the WD and the spectrogram

plane. Consider the fractional FT of  $x(t)$ , denoted by  $X^\alpha(u)$  [Articles 4.8, 5.9]. Its STFT is

$$F_x^\alpha(u, v) = \int_{-\infty}^{\infty} X^\alpha(u+\tau)h(\tau) \exp(-j2\pi v\tau) d\tau. \quad (8)$$

where  $h(\tau)$  is the lag window. The SM in the fractional domain, is defined by

$$SM_x^\alpha(u, v) = 2 \int_{-\infty}^{\infty} P(\theta) F_x^\alpha(u, v + \theta) F_x^{\alpha*}(u, v - \theta) d\theta, \quad (9)$$

It can be easily realized based on the signal's fractional FT and (8).

Using the STFT rotational property,  $F_x^\alpha(u, v) \exp(-j\pi uv) = F_x^0(t, f) \exp(-j\pi t f)$  with  $u = t \cos \alpha + f \sin \alpha$ ,  $v = -t \sin \alpha + f \cos \alpha$ , [12], we can rewrite (9) as

$$SM_x^\alpha(t, f) = 2 \int_{-\infty}^{\infty} P(\theta) F_x^0(t - \theta \sin \alpha, f + \theta \cos \alpha) \times F_x^{0*}(t + \theta \sin \alpha, f - \theta \cos \alpha) e^{j4\pi f \theta \sin \alpha} d\theta, \quad (10)$$

For  $\alpha = 0$  it gives (4), while (7) follows for  $\alpha = -\pi/2$ . For the derivation of (10) the lag window  $h(\tau)$  is formally assumed as  $(W^\alpha(-\tau))^*$ . Optimal direction for the fractional SM calculation can be obtained based on the fractional moments analysis in [Article 4.8]. It has been used in [12].

**Affine SM form:** Continuous wavelet transform (WT) is defined by  $D_x(t, f) =$

$\int_{-\infty}^{\infty} x(\tau)h^*((\tau - t)f/f_0) d\tau / \sqrt{|f_0/f|}$ . As in [3] we used frequency instead of scale  $a = f_0/f$ . Consider  $h(t)$  in the form  $h(t) = w(t) \exp(j2\pi f_0 t)$  which provides a strong formal connection of the WT with the STFT. The pseudo affine Wigner distribution is defined by

$$W_x^a(t, f) = \int_{-\infty}^{\infty} w(\frac{\tau}{2f_0} f) w(-\frac{\tau}{2f_0} f) \times x(t + \frac{\tau}{2}) x^*(t - \frac{\tau}{2}) e^{-j2\pi \tau f} d\tau. \quad (11)$$

The affine SM form reads:

$$SM_x^a(t, f) = 2 \int_{-\infty}^{\infty} P(\theta) D_x(t, f; f_0 + \theta) D_x^*(t, f; f_0 - \theta) d\theta, \quad (12)$$

where  $D_x(t, f; f_0 + \theta)$  is the WT calculated with  $h(t) = w(t) \exp(j2\pi(f_0 + \theta)t)$ . If  $P(\theta) = \delta(\theta)/2$ , then  $SM_x^a(t, f)$  is equal to the scalogram of  $x(t)$ , while for  $P(\theta) = 1$  it produces  $W_x^a(t, f)$  defined by (11). This form of the SM has been extended to other time-scale representations in [3].

*B. Discrete Realization of the Basic S-Method Form*

Discrete SM, for a rectangular window  $P(\theta)$ , follows from (4)

$$SM_x(n, k) = \frac{2}{T_w} [|F_x(n, k)|^2 + 2Re\{\sum_{i=1}^{L_P} F_x(n, k + i) F_x^*(n, k - i)\}] \quad (13)$$

where:  $F_x(n, k) = DFT_{i \rightarrow k}\{x(n+i)w(i)\Delta t\}$ ,  $\Delta t$  is the sampling interval,  $T_w = N\Delta t$  is the width of  $w(\tau)$ , and  $2L_P + 1$  is the width of  $P(\theta)$  in the discrete domain. For notation simplicity we will assume normalized  $2/T_w = 1$ . Recursive relation for the SM calculation is

$$SM_x(n, k; L_P) = SM_x(n, k; L_P - 1) + 2Re\{F_x(n, k + L_P)F_x^*(n, k - L_P)\} \quad (14)$$

where  $SM_x(n, k; 0) = |F_x(n, k)|^2$ , and  $SM_x(n, k; L_P)$  denotes  $SM_x(n, k)$  in (13) calculated with  $L_P$ . In this way we start from the spectrogram, and gradually make the transition toward the WD. The calculation in (13) and (14) needn't be done for each point  $(n, k)$  separately. It can be performed for the whole matrix of the SM and the STFT. This can significantly save time in some matrix based calculation tools. In the SM calculation: 1) There is no need for analytic signal calculation since the cross-terms between negative and positive frequency components are removed in the same way as are the other cross-terms [10]. 2) If we take that  $F_x(n, k) = 0$  outside the basic period, i.e., when  $k < -N/2$  or  $k > N/2 - 1$ , then there is no aliasing when the STFT is alias-free (in this way we can calculate the alias-free WD by taking  $L_P = N/2$  in (13)).

For the SM realization we have to implement the STFT first, based either on the FFT routines or recursive approaches suitable for hardware realizations [6], [10]. After we get the STFT we have to "correct" the obtained values, according to (13), by adding few terms  $2Re\{F_x(n, k+i)F_x^*(n, k-i)\}$  to the SPEC values.

There are two possibilities to implement the summation in (13):

- 1) With a signal independent  $L_P$ . Theoretically, in order to get the WD for each individual component, the length  $L_P$  should be such that  $2L_P$  is equal to the width of the widest auto-term. This will guarantee cross-terms free distribution for all components which are at least  $2L_P$  samples apart. For components and time instants where this condition is not satisfied, the cross-terms will appear, but still in a reduced form (see also [Article 7.3]).
- 2) With a signal dependent  $L_P = L_P(n, k)$  where the summation, for each point  $(n, k)$ ,

lasts until the absolute square value of  $F_x(n, k+i)$  or  $F_x(n, k-i)$  is smaller than an assumed reference level  $R$ . If a zero value may be expected within a single auto-term, then the summation lasts until two subsequent zero values of  $F_x(n, k+i)$  or  $F_x(n, k-i)$  are detected. The reference level is defined as a few percent of the spectrogram's maximal value at a considered instant  $n$ ,  $R_n = \max_k\{S_x(n, k)\}/Q^2$ , where  $Q$  is a constant. Index  $n$  is added to show that the reference level  $R$  is time dependent. Note that if  $Q^2 \rightarrow \infty$ , the WD will be obtained, while  $Q^2 = 1$  results in the spectrogram. A choice of an appropriate value for design parameter  $Q^2$  will be discussed in *Example 2*.

*Example 1:* Consider a real-valued multi-component signal

$$x(t) = \cos(1200(t + 0.1)^2) + e^{-36(t-1/3)^2} \cos(1200(t+1/2)^2) + e^{-36(t-2/3)^2} \cos(1200(t-1/3)^2) + \cos(960\pi t)$$

within the interval  $[0, 1]$ , sampled at  $\Delta t = 1/1024$ . This sampling rate is very close to the Nyquist rate for this signal, that is  $1/960$ . The Hanning window of the width  $T_w = 1/4$  is used. The spectrogram is shown in Fig.2(a). Its "corrected" version (the SM), according to (13), with five terms,  $L_P = 5$ , is shown in Fig.2(c). The auto-terms are concentrated almost as in the WD, Fig.2(b). The Choi-Williams distribution (CWD), whose kernel reads  $c(\nu, \tau) = \exp(-(\nu\tau)^2)$ , is shown in Fig.2(d). Normalized values  $-\sqrt{\pi N/2} \leq |2\pi\nu| \leq \sqrt{\pi N/2}$ ,  $-\sqrt{\pi N/2} \leq |\tau| \leq \sqrt{\pi N/2}$ , and 128 samples within that interval, are used. If the analytic part of  $x(t)$  were used, similar results would be obtained, see [Article 9.1, Fig.1].

*Example 2:* The adaptive SM realization will be illustrated on a three-component real signal, with a nonlinear FM component,

$$x(t) = e^{-t^2} \cos(25\pi t) + \cos(120t^3 + 45\pi t) + 1.5e^{-25t^2} \cos(40\pi t^2 + 150\pi t)$$

with the sampling interval  $\Delta t = 1/256$ . The signal is considered within the time interval

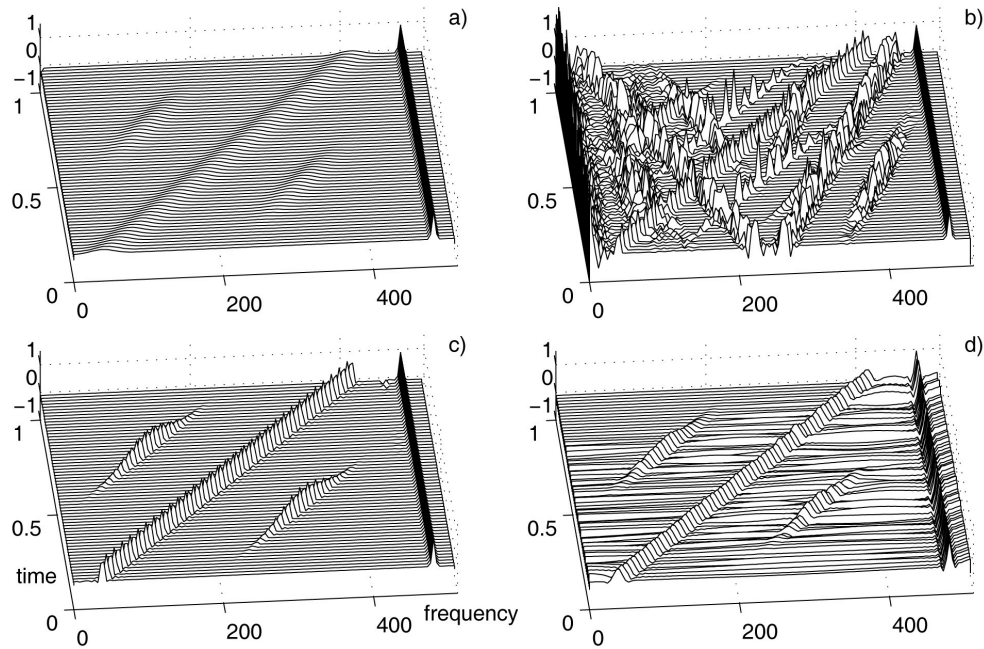


Fig. 2. Time-frequency representation of a real-valued multicomponent signal: a) Spectrogram, b) Pseudo Wigner distribution, c) S-method with five "correcting terms",  $L_P = 5$ , d) Choi-Williams distribution, as the representative of reduced interference distributions.

$[-1, 1]$ . The Hanning window of the width  $T_w = 1$  is used. The spectrogram is presented in Fig.3(a), while the SM with the constant  $L_P = 3$  is shown in Fig.3(b). The concentration improvement with respect to the case  $L_P = 0$ , Fig.3(a), is evident. Further increase of  $L_P$  would improve concentration, but it would also cause that some cross-terms appear. Some small changes are already noticeable between the components with quadratic and constant IF. An improved concentration, without cross-terms, can be achieved by using the variable window width  $L_P$ . The regions  $D_i(n, k)$ , determining the summation limit  $L_P(n, k)$  for each point  $(n, k)$ , are obtained by imposing the reference level  $R_n$  corresponding to  $Q^2 = 50$ . They are defined as:  $D_i(n, k) = 1$  when  $S_x(n, k) \geq R_n = \max_k \{S_x(n, k)\} / Q^2$ , and  $D_i(n, k) = 0$  elsewhere, Fig.3(c). White regions mean that the value of spectrogram is below 2% of its maximal value at that time instant  $n$ , meaning that the concentration improvement is not performed at these points. The signal dependent SM is given in Fig.3(d).

The method sensitivity, with respect to the value of  $Q^2$ , is low.

### C. STFT Based Realization of Higher Order Representations

In order to improve distribution concentration in the case of nonlinear FM signals, the higher order time-varying spectra have been defined (Wigner higher order spectra, Multi-time Wigner distributions). For practical realizations the most interesting are the versions of these spectra reduced to the two-dimensional TF plane [4]. Here, we will present the L-Wigner distribution (LWD) and the fourth order polynomial Wigner-Ville distribution (PWVD).

#### C.1 The L-Wigner Distribution

The L-Wigner Distribution (LWD) is defined by [8], [10]

$$LD_L(t, f) =$$

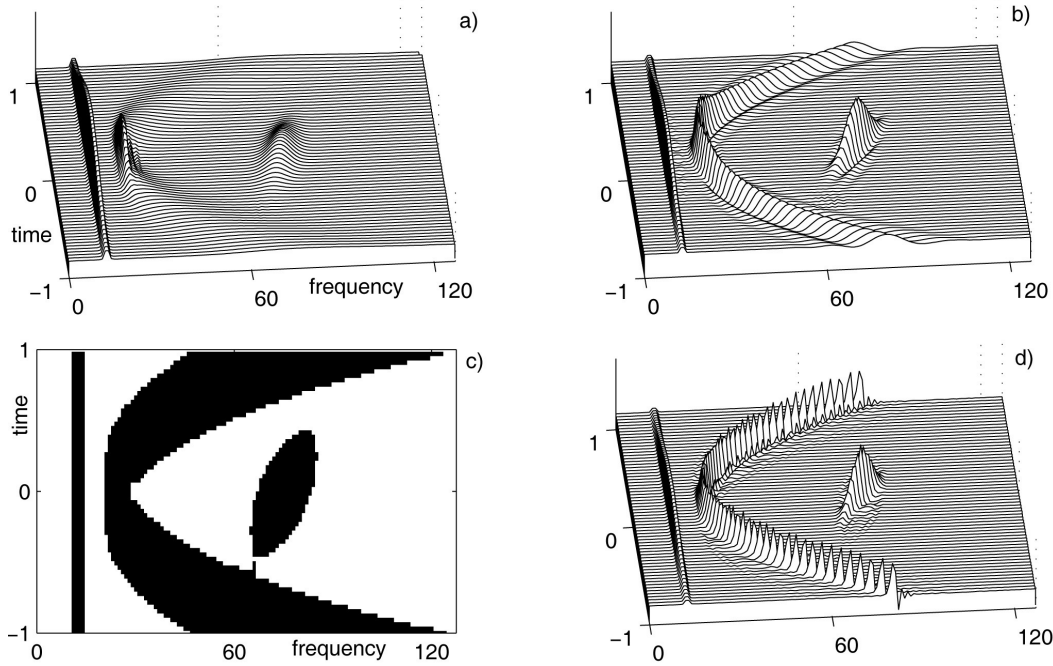


Fig. 3. Time-frequency analysis of a multicomponent signal: a) Spectrogram, b) The S-method with a constant window, with  $L_P = 3$ , c) Regions of support for the S-method with a variable window width calculation, corresponding to  $Q^2 = 50$ , d) The S-method with the variable window width calculated using regions in c).

$$\int_{-\infty}^{\infty} w_L(\tau)x^{*L}(t - \frac{\tau}{2L})x^L(t + \frac{\tau}{2L})e^{-j2\pi f\tau} d\tau. \tag{15}$$

For  $L = 1$  it reduces to the WD.

The LWD is a windowed slice of the multi-time Wigner distributions:

$$W_x^K(t_1, \dots, t_k, f) = \int_{-\infty}^{\infty} x^*(\sum_{i=1}^K t_i + \frac{\tau}{K+1}) \prod_{i=1}^{L-1} x^*(-t_i + \frac{\tau}{K+1}) \times \prod_{i=L}^K x(t_i - \frac{\tau}{K+1}) e^{j2\pi f\tau} d\tau,$$

along the line  $t_1 = t_2 = \dots = t_{L-1} = -t$ ,  $t_L = t_{L+1} = \dots = t_K = t$ , where the auto-terms in  $W_x^K(t_1, \dots, t_k, f)$  are located, for  $L = (K+1)/2$  [8].

Similarly, starting from the Wigner higher order spectra, dual to  $W_x^K(t_1, t_2, \dots, t_k, f)$ , we get a distribution dual to (15),

$$LW_L^f(t, f) =$$

$$\int_{-\infty}^{\infty} W_L(\theta)X^{*L}(f + \frac{\theta}{2L})X^L(f - \frac{\theta}{2L})e^{-j2\pi\theta t} d\theta. \tag{16}$$

studied in details in [7]. Its realization is formally the same as for the time domain LWD.

For a frequency modulated signal  $x(t) = \exp(j\phi(t))$ , the LWD produces [10]

$$LW_L(t, f) = W_L(f - \phi'(t)/2\pi) *_f FT\{e^{j(\phi^{(3)}(t+\tau_1)+\phi^{(3)}(t-\tau_2))/(48L^2)}\},$$

where  $\tau_1, \tau_2$  are the values of  $\tau$  within the lag window  $w_L(\tau)$ , and  $W_L(f) = \mathcal{F}_{\tau \rightarrow f}\{w_L(\tau)\}$ . For  $L \rightarrow \infty$ , the LWD tends to a distribution completely concentrated along the IF, i.e.,  $LW_L(t, f) \rightarrow W_L(f - \phi'(t)/2\pi)$ .

The relationship between  $LW_{2L}(t, f)$  and  $LW_L(t, f)$  is of form (3),

$$LW_{2L}(t, f) = 2 \int_{-\infty}^{\infty} LW_L(t, f + \theta)LW_L(t, f - \theta)d\theta$$

The realization of cross-terms and alias free version of the LWD may be efficiently done in the discrete domain, by using the SM form (13), as:

$$LW_{2L}(n, k) = LW_L^2(n, k) + 2 \sum_{i=1}^{L_P} LW_L(n, k+i) LW_L(n, k-i), \quad (17)$$

with  $LW_1(n, k) = W_x(n, k)$ , and  $W_x(n, k)$  calculated according to (13). Form (17) is very convenient for software and hardware realizations since the same blocks, connected in cascade, can provide a simple and efficient system for higher order TF analysis, based on the STFT in the initial step, and the signal sampled at the Nyquist rate. Numerical examples and illustrations of the LWD can be found in [7]-[10].

### C.2 Polynomial Wigner-Ville Distribution

Modification of the presented method for the realization of the PWVD is straightforward. The fourth order PWVD can be written in a frequency scaled form [2]

$$PW_x(t, f) = \frac{1}{2.7} \int_{-\infty}^{\infty} x^2(t + \frac{\tau}{4}) x^{*2}(t - \frac{\tau}{4}) \times x^*(t + A\frac{\tau}{2}) x(t - A\frac{\tau}{2}) e^{-j\frac{2\pi f}{2.7}\tau} d\tau, \quad (18)$$

where  $A = 0.85/1.35$  and  $f' = f/2.7$ . Note that  $PW_x(t, f') = \frac{1}{2.7} LW_2(t, f') *_{f'} W_x^A(t, f')$ , where  $W_x^A(t, f') = FT\{x^*(t + A\frac{\tau}{2})x(t - A\frac{\tau}{2})\}$  is the scaled and reversed version of the WD. The cross-terms free realization of the WD and LWD is already presented. In the discrete implementation of the above relation, the only remaining problem is the evaluation of  $W_x^A(t, f')$  on the discrete set of points on frequency axis,  $f' = -k\Delta f'$ . Since  $W_x^A(t, f')$  is, by definition, a scaled and reversed version of  $W_x(t, f')$ , its values at  $f' = -k\Delta f'$  are the values of  $W_x(t, f')$  at  $f' = k\Delta f'/A$ . However, these points do not correspond to any sample location along the frequency axis grid. Thus, the interpolation has to be done (one way of doing it is in an appropriate zero padding of the signal). A discrete form of convolution (18), including rectangular window  $P(\theta)$  and the above considerations, is

$$PW_x(n, k) =$$

$$\sum_{i=-L_P}^{L_P} LW_2(n, k+i) \hat{W}_x(n, k+i/A) \quad (19)$$

where  $2L_P + 1$  is the width of  $P(\theta)$  in the discrete domain, while  $\hat{W}_x(n, k+i/A)$  is the WD approximation. We can simply use  $\hat{W}_x(n, k+i/A) = SM_x(n, k+[i/A])$  where  $[i/A]$  is the nearest integer to  $i/A$ , or use the linear interpolation of the SM values at two nearest integers. The terms in (19), when  $k+i$  or  $k+[i/A]$  is outside the basic period, are considered as being zero in order to avoid aliasing.

*Example 3:* Consider real-valued multicomponent signal

$$x(t) = \cos(20 \sin(\pi t) + 30\pi t) + \sin(20 \cos(\pi t) + 100\pi t)$$

within  $-1 \leq t < 1$ , with  $\Delta t = 1/128$ . In the realization, a Hanning window of the width  $T_w = 2$  is used. Based on the STFT (using its positive frequencies), the cross-terms free WD is obtained from (13) with  $L_P = 15$ , and denoted by SM, Fig.4(a). Then the LWD, with  $L = 2$ , is calculated according to (17). It is combined with the linearly interpolated SM value into the PWVD (19), shown in Fig.4(b). For the precise implementation of  $[i/A]$  the lag window has been zero-padded by a factor of 2.

### D. Summary

The STFT based realization of quadratic TF representations, having the auto-terms close or the same to the ones in the WD, but without (or with reduced) cross-terms, is presented. For this realization the S-method is used. The method is generalized, in an order recursive form, for the realization of higher order TF representations. Applications of the presented method on, for example, time-scale representations [3], and multidimensional space/spatial-frequency analysis [14], are straightforward. Hardware realization of the S-method is also simple and direct [10].

### REFERENCES

- [1] L. Cohen, *Time-frequency analysis*, Prentice-Hall, 1995.
- [2] B. Boashash and B. Ristic, "Polynomial time-frequency and time-varying higher order spectra: Application to the analysis of multicomponent FM signals and to the treatment of multiplicative noise," *Sig. Proc.*, vol.67, pp.1-23, 1998.

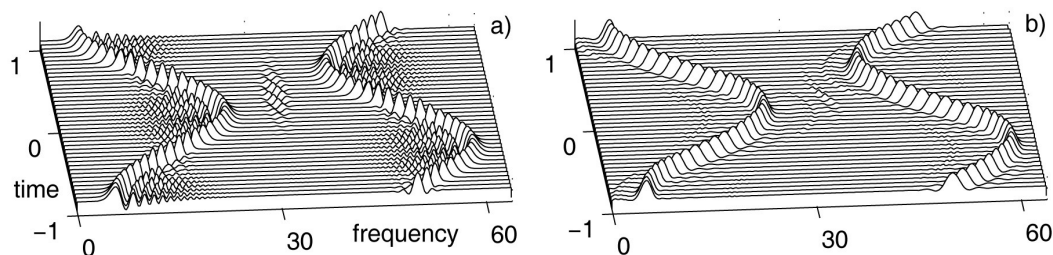


Fig. 4. Time-frequency representation of a real-valued multicomponent signal: a) The SM (cross-terms and alias free version of the WD), b) Polynomial Wigner-Ville distribution realized based on the STFT by using the SM and its order recursive form.

- [3] P. Gonçalves and R.G. Baraniuk, "Pseudo affine Wigner distributions: Definition and kernel formulation," *IEEE Trans. SP*, vol.46, pp.1505-1517, June 1998.
- [4] B. Ristic and B. Boashash, "Relationship between the Polynomial and Higher order Wigner-Ville distribution," *IEEE SP Letters*, vol.2, pp.227-229, Dec.1995.
- [5] L.L. Scharf and B. Friedlander, "Toeplitz and Hankel kernels for estimating time-varying spectra of discrete-time random processes," *IEEE Trans. SP*, vol.49, pp. 179-189, Jan. 2001.
- [6] L.J. Stanković, "A method for time-frequency analysis," *IEEE Trans. SP*, vol.42, pp. 225-229, Jan.1994.
- [7] L.J. Stanković, "An analysis of Wigner higher order spectra of multicomponent signals," *Ann. Telecomm.*, no.3/4, pp.132-136, Mar./Apr. 1994.
- [8] L.J. Stanković, "Multitime definition of the Wigner higher order distribution: L-Wigner distribution," *IEEE SP Letters*, vol.1, no.7, pp.106-109, July 1994.
- [9] L.J. Stanković, "An analysis of some time-frequency and time-scale distributions," *Ann. Telecomm.*, vol.49, no.9/10, pp.505-517, Sep./Oct.1994.
- [10] L.J. Stanković, "A method for improved distribution concentration in the time-frequency analysis of the multicomponent signals using the L-Wigner distribution", *IEEE Trans. SP*, vol.43, pp.1262-1268, May 1995.
- [11] L.J. Stanković, "The auto-term representation by the reduced interference distributions; The procedure for a kernel design," *IEEE Trans. SP*, vol.44, pp.1557-1564, June 1996.
- [12] L.J. Stanković, T. Alieva and M. Bastiaans, "Fractional Fourier-domain weighted Wigner distribution," in *Proc. 11th IEEE WSSP*, Singapore, pp.321-324, Aug. 2001.
- [13] L.J. Stanković and J.F. Böhme, "Time-frequency analysis of multiple resonances in combustion engine signals," *Sig. Proc.*, vol.79, no.1, pp.15-28, Nov.1999.
- [14] S. Stanković, L.J. Stanković and Z. Uskoković, "On the local frequency, group shift, and cross-terms in some multidimensional time-frequency distributions; A method for multidimensional time-frequency analysis," *IEEE Trans. SP*, vol.43, pp.1719-1725, July 1995.